

# The ferroelastic phase transition and non-180° domain switching in La-modified lead zirconate titanate ferroelectric ceramics

Can Wang<sup>1,2</sup>, Simon A T Redfern<sup>1</sup>, Fernando Aguado<sup>1,3</sup> and Maren Daraktchiev<sup>1</sup>

<sup>1</sup> Department of Earth Sciences, University of Cambridge, Downing Street, Cambridge CB2 3EQ, UK

<sup>2</sup> Institute of Physics, Chinese Academy of Sciences, Beijing 100190, People's Republic of China

Received 22 January 2009, in final form 11 June 2009

Published 29 June 2009

Online at [stacks.iop.org/JPhysCM/21/295901](http://stacks.iop.org/JPhysCM/21/295901)

## Abstract

The ferroelastic phase transition and shape memory effect in La-modified lead zirconate titanate ferroelectric ceramics are demonstrated directly through the temperature-dependent macroscopic recoverable strain measured in a three-point bending configuration. X-ray diffraction measurements reveal that non-180° domain switching occurs in the mechanically poled sample in two different ways at the bottom and top of the sample which have been under tensile and compressive stresses, respectively. The calculated fraction of non-180° switched domains in the poled sample increases nonlinearly with the applied force and shows a saturation trend, which is consistent with the nonlinear behavior of the remnant strain. This study confirms that the mechanical stress applied upon cooling ferroelectric ceramics from the paraelectric to the ferroelectric phase can easily activate ferroelastic domain switching and give rise to preferred domain orientation and consequent macroscopic remnant strain which results in a history effect and shape memory effect via the ferroelastic phase transition.

(Some figures in this article are in colour only in the electronic version)

## 1. Introduction

Ferroelectric materials are widely used in various electrical and mechanical devices for their piezoelectric and ferroelectric properties. In ferroelectric perovskite materials, such as barium titanate, BaTiO<sub>3</sub>, and lead zirconate titanate, Pb(ZrTi)O<sub>3</sub> (PZT), upon cooling through the Curie temperature ( $T_C$ ), domain structures are formed to minimize the free energy during the structural transition from cubic to the tetragonal or rhombohedral phase, and the materials become spontaneously electrically polarized and mechanically distorted. The polar direction of domains can be reorientated through either 180° reversal or non-180° rotation under external electric or mechanical field, respectively, resulting in changes in electric polarization and remnant strain. External

electric field can induce both 180° and non-180° domain switching, however mechanical stress can only induce non-180° domain switching. The 180° domain switching is pure ferroelectric and contributes only to the electric polarization, but the non-180° domain switching can give rise to a remnant strain which is the signature of ferroelasticity. The non-180° domain switching is distortive in character and the structural phase transition of ferroelectric materials at  $T_C$  is apt to show coupling between ferroelastic and ferroelectric order parameters. The study of non-180° domain switching in ferroelectrics has attracted much attention because of the significant influence of non-180° domain switching on the electromechanical properties of ferroelectric materials [1–3]. Moreover, studies have shown that dynamic mechanical stress applied to ferroelectrics can result in some novel properties such as flexoelectric and thermoelastic effects [4, 5], and especially stress or strain on ferroelectric or multiferroic

<sup>3</sup> Present address: DCITIMAC, Facultad de Ciencias, Universidad de Cantabria, Santander 39005, Spain.

thin films can give a distinct change of their physical properties [6–8].

Non-180° domain switching can be characterized by x-ray diffraction fairly easily, because the non-180° switching of the polar axis will generally induce a change in the relative dimensions of the unit cell, which is discernible by diffraction techniques. Rogan *et al* [9] have employed neutron diffraction to analysis the ferroelastic domain switching of PZT ceramics under compressive stress. Synchrotron x-ray and laboratory x-ray diffractions are also effective in characterizing the non-180° domain reorientation in PZT ceramics [10–17]. Guo *et al* [18] have reported direct evidence for the origin of high piezoelectricity in PZT by x-ray diffraction measurements.

The ferroelasticity of PZT ceramics has been revealed by stress–strain measurements [19]; whereas, the mechanical poling resulting from applying stress during a ferroelastic phase transition and its influence on non-180° domain switching are rarely mentioned. Particularly, in La-modified PZT (65/35) ceramics, when the La content rises over 4%, the phase transition becomes more diffusive because of the appearance of polar nanoclusters in the ceramic and the material is regarded as a relaxor ferroelectric which exhibits very different behavior compared to a normal ferroelectric [20]. We have reported the effect of ferroelastic domain switching on the dynamic modulus and mechanical loss of a rhombohedral PZT ceramic [21] and the discontinuous temperature-dependent macroscopic strain due to ferroelastic domain switching and structural phase transitions in barium strontium titanate [22]. In this paper, we report a direct observation of the ferroelastic phase transition and induced shape memory effect based on the measurements of temperature-dependent remnant strain in La-modified PZT ceramics, and give an analysis of non-180° domain switching in the mechanically poled sample by x-ray diffraction measurement. Moreover, the mechanism of ferroelastic domain switching during mechanical poling is discussed.

## 2. Experiment

The ceramics used in this study are La-modified PZT with formula  $\text{Pb}_{1-x}\text{La}_x(\text{Zr}_{0.65}\text{Ti}_{0.35})_{1-x/4}\text{O}_3$  (PLZT), and La content of 0.01, 0.05, and 0.07, which are denoted as PLZT01, PLZT05, and PLZT07, respectively. The PZT ceramics, synthesized by solid state reaction techniques, were sintered in a hot-press furnace under oxygen atmosphere. The samples, cut by a diamond cutting system, were about  $0.6 \times 3 \times 12 \text{ mm}^3$  in size. A Perkin-Elmer dynamical mechanical analyzer (DMA-7e) was used to measure the remnant strain via bending deformation in three-point bending (TPB) configuration, and also to measure the dynamic modulus and mechanical loss. The sample was supported on two parallel knife edges 10 mm apart, and a force composed of a static and a dynamic component was applied on the center of the sample via a probe using an electromechanical force motor. The static force was set to be 110% of the dynamic force  $F$ , so that the sample was always under a mechanical bias. The maximum stress  $\sigma_m$  on a bending sample can be calculated by  $\sigma_m = 3Fl/2t^2w$  ( $l = 10 \text{ mm}$ ,  $w = 3 \text{ mm}$ ,  $t = 0.6 \text{ mm}$ ), so for 100 mN

force applied on our sample the  $\sigma_m$  is roughly about 1.5 MPa. Both the tube of the sample holder and the probe rod were made of quartz, which was essential to avoid possible artifacts due to their thermal expansion during the thermal cycle. The probe position ( $\mu$ ) can be recorded by electromagnetic inductive coupling with a resolution of 10 nm. The value of static bending deformation,  $d(T)$ , is determined by the absolute value of the difference between the probe position at a temperature  $T$  and a given high temperature (which is 400, 300, and 250 °C, for the three samples with different La content, respectively) at which the sample is in the paraelectric phase. Corresponding to 1  $\mu\text{m}$  bending deformation, the maximum tensile strain at the bottom of our sample is about  $2 \times 10^{-5}$ . The tensile strain is defined by the sample thickness divided by  $2R$  ( $R$  is the bending radius of the sample). The remnant strain in this study is represented by the value of the static bending deformation. The bending deformation consists of a large remnant strain, which remains when the applied force is removed, plus a small induced elastic component, which is related to the difference of the modulus between ferroelectric and paraelectric phases and is only present in the ferroelectric phase when a force is applied. All measurements of the temperature-dependent remnant strain have been performed at a temperature ramp rate of  $10 \text{ K min}^{-1}$ .

In this study, mechanical poling means that only mechanical stress is applied on the ferroelectric sample to obtain domain reorientation, and such mechanical poling is performed by applying a 10 Hz dynamic stress on the sample upon cooling through para-ferroelectric phase transition to room temperature. Initially, each sample was annealed at 400 °C to get rid of the possible texture and residual stress from the cutting process ('initial sample'), and 'a mechanically poled sample' refers to any sample has undergone a mechanical poling process.

X-ray diffraction measurements were performed using a Bruker D8 advance x-ray diffractometer using  $\text{Cu K}\alpha_1$  radiation in slow scanning at  $0.3^\circ \text{ min}^{-1}$ , and the sample's bottom or top surface was set to be perpendicular to the scattering plane which contains the incident and diffractive x-ray beams. The intensity of the reflections was determined by fitting the experimental results with the software Fullprof.

## 3. Characterization of non-180° domain switching by x-ray diffraction

Friedel's law requires that intensities at reciprocal space points related by inversion (for example,  $hkl$  and  $\bar{h}\bar{k}\bar{l}$ ) be equal, so in general a 180° reversion of a unit cell have no effect on the x-ray intensity. Here, it would be mentioned that Friedel's law breaks down when dispersion corrections are taken into account, and the Bijvoet difference can be enhanced via use of x-ray energies close to an absorption edge [23]. Under this conditions, Do *et al* has observed a 30% change in the intensity of PZT reflections upon reversal of polarization [24]. In our case, only non-180° domain switching can occur under mechanical stress, and furthermore our measurements were made well away from any absorption edge and the imaginary part of the atomic scattering factors were negligible. In these circumstances any variation of the x-ray intensity would not

be associated with 180° domain switching. However, when a unit cell is reoriented by a non-180° angle, local switching of the dimensions of the unit cell will result, and then x-ray diffraction from the unit cell will be influenced. Accordingly, non-180° domain switching can be characterized by measuring x-ray diffraction in terms of the intensity variation of the Bragg peaks for the planes perpendicular to the possible polar axes. For a tetragonal ferroelectric, the polar axis is parallel to the [001] crystallographic direction and under external stress it could be reorientated by 90° switching to be along [100] or [010], hence the intensity ratio  $I_{(100)}/I_{(001)}$  is sensitive to 90° domain switching. For a rhombohedral ferroelectric, the dipole formed due to ion displacement lies along the [111] direction of the pseudocubic unit cell [22]. Under external mechanical stress, the polar axis can be switched among the four possible directions by either 71° or 109° and consequently the x-ray diffraction intensities of the reflections (111) and (11 $\bar{1}$ ) will be modified. Therefore, non-180° switching in rhombohedral ferroelectric ceramics can be inferred from the variation of the intensity ratio  $I_{(11\bar{1})}/I_{(111)}$ .

Non-180° domain switching can be quantified by the x-ray diffraction measurement. Subbarao *et al* [25] have developed a model in terms of the intensity ratios to calculate the per cent of 90° switched domains in tetragonal BaTiO<sub>3</sub> ceramics, and subsequently many studies have been carried out to investigate the 90° domain switching in tetragonal ferroelectric ceramics by x-ray diffraction [14–16], but thus far only a few studies have reported non-180° domain switching in rhombohedral ferroelectrics [12, 17]. There has been some confusion in the reported studies because the quantification of domain switching by x-ray diffraction depends not only on the structure of the materials but also on the configuration of x-ray measurement and external field. The ceramics used in this study are in the rhombohedral ferroelectric phase. The bottom and top regions of the mechanical poled sample experience tensile and compressive stresses, respectively, and the surface used for x-ray diffraction analysis is parallel to the direction of the stresses. To calculate the per cent of non-180° switched domains in a mechanically poled sample, we have derived an expression that quantitatively relates the intensity ratios of diffraction peaks to the degree of domain switching in the rhombohedral phase, following the methods previously adopted for tetragonal ferroelectrics [15, 25].

The relative intensities of the different reflections of a polycrystalline ceramic can be described as:

$$I_{hkl} = C P_{hkl} F_{hkl}^2 L_{hkl}(\theta) e^{-2M} W_{hkl} \quad (1)$$

where,  $C$  is a constant related to experimental conditions,  $L_{hkl}$  is the Lorentz-polarization factor,  $F_{hkl}$  is the structure factor,  $P_{hkl}$  the multiplicity factor,  $e^{-2M}$  is the temperature factor, and  $W_{hkl}$  is the diffraction probability of  $(hkl)$  crystal planes in the area that is capable of reflection. For a rhombohedral ferroelectric ceramic, the intensity  $I_{(111)}$  arises from the domains with their polar axis [111] perpendicular to the sample surface and the intensity  $I_{(11\bar{1})}$  is due to domains with one of their  $\langle 11\bar{1} \rangle$  directions perpendicular to the sample surface. The difference of the Lorentz-polarization factors, thermal factors and structure factors can be neglected for

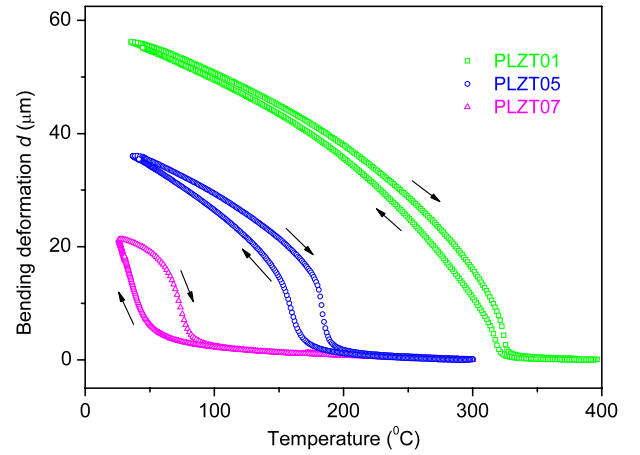


**Figure 1.** Bending deformation as a function of temperature for PLZT01, PLZT05 and PLZT 07, measured with 200 mN applied force during cooling and subsequent heating.

the reflections of (111) and (11 $\bar{1}$ ), and in rhombohedral ferroelectrics  $P_{11\bar{1}}$  is 6 and  $P_{111}$  is 2. Then, from equation (1), the intensity ratios for an unpoled and a tensile stressed sample are  $R = I_{(11\bar{1})}/I_{(111)} = 3W_{(11\bar{1})}/W_{111}$  and  $R' = I'_{(11\bar{1})}/I'_{(111)} = (3W_{(11\bar{1})}/W_{111} + N)/(1 - N)$ , respectively. Here,  $N$  represents the fraction of the domains (with polar axis perpendicular to the sample surface) that switch their polar axes from being perpendicular to the surface into other possible polar directions via 71° or 109° reorientations under tensile stress. According to the expression of  $R$  and  $R'$ ,  $N$  can be expressed as  $N = (R' - R)/(1 + R')$ . Then, the fraction of non-180° domains that switch under tensile stress is given by the ratio of the switched domains to the total number of domains:

$$\eta = \frac{N P_{111} W_{111}}{P_{111} W_{111} + P_{11\bar{1}} W_{11\bar{1}}} = \frac{R' - R}{(1 + R)(1 + R')} \quad (2)$$

where,  $R$  and  $R'$  can be measured by x-ray diffraction on an initial and a poled sample. In the same way, without regard to the sign, an identical formula can be obtained for the case of compressive stress. So, equation (2) is suitable for both the cases of tensile and compressive stresses, but the calculated fractional value  $\eta$  for compressive stress is negative because the value of  $R'$  is less than that of  $R$  in the case of a compressive stress. Here, the calculated fraction of non-180° switched domains excludes the possible switching of polar axis among the directions of  $\langle 11\bar{1} \rangle$ . In addition, this formula is also suitable for calculating the volume fraction of non-180° domains in an electrically poled ferroelectric sample.

## 4. Results and discussion

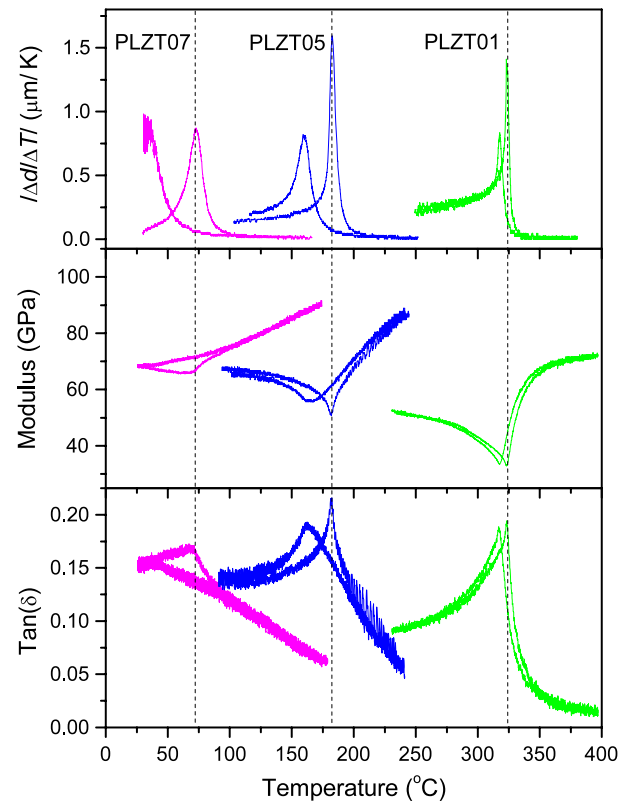
### 4.1. Temperature-dependent remnant strain

Figure 1 shows the remnant strain (represented by bending deformation) as a function of temperature for three PZT samples of different composition. The result for each sample was measured by applying 200 mN force on the sample during a thermal cycle starting with cooling from high temperature

to room temperature and then heating back. On cooling the bending deformation appears abruptly at the ferroic phase transition and then increases gradually with further decreasing temperature. On subsequent heating, the bending deformation for each sample goes back down and then collapses completely to zero at high temperature. The complete recoverability of the bending deformation implies that the bending stress applied during the experiment is lower than the limit for dislocation-mediated plastic strain of the material and the deformation is due to recoverable remnant strain by ferroelastic domain switching. The temperature-dependent remnant strain is completely repeatable in subsequent thermal cycles when using an identical force. The abrupt increase and the collapse of remnant strain demonstrate directly a para-ferroelastic phase transition on cooling and a reverse ferro-paraelastic phase transition on heating. The temperature, where the remnant strain dramatically changes, indicates the Curie temperature for the ferroic phase transition.

For PLZT01, which is a normal ferroelectric, the structural phase transition on cooling is from cubic to rhombohedral, which is a para-ferroelectric with coupled para-ferroelastic phase transition behavior. The situation in respect to the relaxor ferroelectrics is slightly more complicated; for PLZT05 and PLZT07, the transition on cooling could be ergodic relaxor to nonergodic relaxor or ergodic relaxor to normal ferroelectric [26]. In the first case, the polar nanoclusters in the relaxor become frozen into a nonergodic state, while the average symmetry of the material remains cubic, thus in this situation no macroscopic remnant strain could appear; furthermore, the nonergodic relaxor state can be irreversibly transformed into a normal ferroelectric state by applying an external electric field. In the second case, the ergodic relaxor transform to a normal ferroelectric phase without external field, and then the realignment of ferroelastic domain can give remnant strain. Accordingly, the evolution of remnant strain with temperature for the two relaxor ferroelectric samples shown in figure 1 proves that the transitions for PLZT05 and PLZT07 on cooling are from ergodic relaxor to normal ferroelectric. Here, the drive for the transition from ergodic relaxor to normal ferroelectric rather than to nonergodic relaxor is the external mechanical poling stress rather than the external electrical field.

Figure 2 shows the rate of change of remnant strain with temperature, the dynamic modulus and mechanical loss as a function of temperature. Here, the modulus and mechanical loss have been measured at 10 Hz and 200 mN dynamic force during the same cooling and heating measurements shown in figure 1. It can be seen that the strain rate maximum, the modulus minimum, and the loss maximum all occur at same temperature in each of the three samples. All these behaviors indicate that domains have higher mobility around the phase transition temperature, and conversely it is suggestive that the high mobility of domains has induced the modulus decrease and the loss increase. The transition temperature obtained on heating is 324, 182, and 72 °C, for PLZT01, PLZT05, and PLZT07, respectively. The large thermal hysteresis behavior between the cooling and heating runs for the two relaxor samples suggests that the relaxor ferroelectrics



**Figure 2.** Remnant strain rate, dynamic modulus, and mechanical loss as a function of temperature for PLZT01, PLZT05 and PLZT07.

undergo a first order phase transition. Moreover, according to the dielectric measurements on PLZT ceramics at 100 kHz during heating reported previously [27], the temperature of the permittivity maximum for PLZT01 is very close to the temperature determined by our low-frequency mechanical measurements, but for the two relaxor ferroelectrics the temperatures determined by our mechanical measurements are much lower than that determined by dielectric measurements. The temperature difference may result from the frequency-dependent behavior in the relaxor ferroelectrics, though the dielectric and mechanical measurements are sensitive to the different responses of electric dipoles and elastic dipoles [28]. The measurement of dynamic modulus and mechanical loss has been used to characterize the phase transitions and inelastic relaxations in PZT based ceramics in many studies [29–32]. The mechanical modulus and loss shown in figure 2 exhibit the different dynamic mechanical behavior for normal and relaxor ferroelectrics. For the normal ferroelectric PLZT01, the modulus and mechanical loss are almost constant at high temperature and the modulus decreases dramatically to its minimum at temperatures very close to the phase transition while the mechanical loss increases to the maximum, correspondingly; but for the two relaxors PLZT05 and PLZT07, the modulus and the mechanical loss vary less rapidly from high temperature to the modulus minimum and the loss maximum, and the variation becomes less abrupt with increasing La content. Under dynamic stress, the polar nanoclusters in relaxor ferroelectrics will give rise to a local ferroelastic response which results in a modulus decrease and a



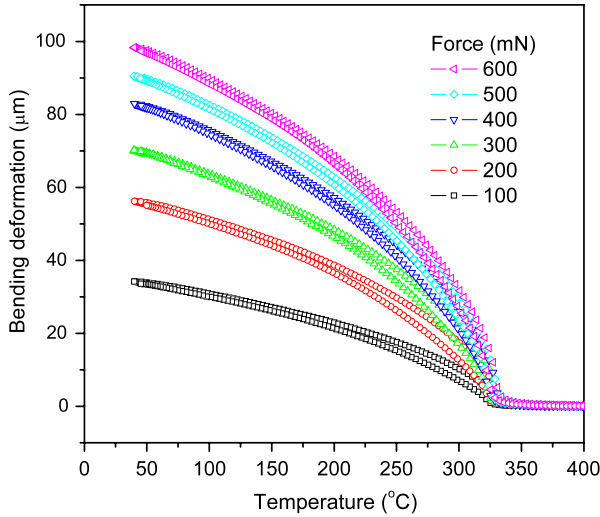


**Figure 3.** Bending deformation as a function of temperature for PLZT01 measured with a range of applied forces from 100 to 600 mN during cooling and subsequent heating.

loss increase. Jimenez *et al* have reported elastic softening due to polar clusters in  $\text{Pb}_{1-x}\text{Ca}_x\text{TiO}_3$  ferroelectric ceramics above the phase transition temperature [33]. Therefore, the gradual variation of the modulus and mechanical loss of the two relaxor ferroelectrics at high temperature most likely reflects the existence and evolution of the polar nanoclusters in the high temperature phase of these materials.

In addition, the temperature dependence of remnant strain also demonstrates a shape memory effect for the PZT ceramics. Generally, a shape memory effect describes the phenomenon where the original shape of a deformed sample is restored by heating via a structural phase transition. The phase transition gives rise to a spontaneous strain by the formation of ferroelastic domains to minimize internal strain energies, and then a larger remnant strain can be easily produced under external stress by rearranging the domains. As shown in figure 1, all the three PZT samples exhibit macroscopic remnant strain by mechanical poling and can completely recover their initial undeformed shape when heated back to the cubic phase. Pandit *et al* have recently reported the shape memory effect in the solid solution of lead magnesium niobate with lead titanate [34, 35]. Similar strain behavior during thermal cycling has been observed by them and the origin of the recoverable strain is explained in terms of the ferroelastic phase transitions and the availability of a large number of competing phases and domain states near the morphotropic phase boundary in the material. Therefore, it would be expected that under applied stress most of the ferroelectric and ferroelastic oxides show macroscopic remnant strain during phase transition between paraelectric and ferroelectric phases, and that the strain can be eradicated by a reverse phase transition. Moreover, because of the coupling between the ferroelastic and ferroelectric properties in ferroelectric materials [35, 36], there is a possibility to control the shape memory effect by using electric field as well as mechanical stress. Related to this, we also note that the shape memory

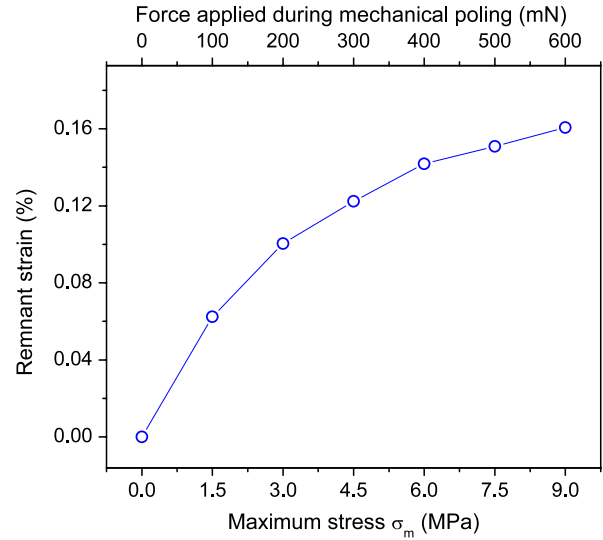


**Figure 4.** Remnant strain at room temperature versus stress for the mechanically poled PLZT01 sample obtained from the result shown in the figure.

effect in some ferroelastic minerals in the mantle of earth could be one of the mediators of seismic energy.

#### 4.2. Force dependence and history effect

In our sample, the variation of remnant strain with temperature is completely repeatable in subsequent thermal runs if the applied force remains unchanged. Now, we turn to relationship between the temperature-dependent remnant strain and the magnitude of the applied force. The temperature dependence of bending deformation has been measured on the PLZT01 sample at various applied forces from 100 to 600 mN, as shown in figure 3. All the measurements are started upon cooling from high temperature to room temperature and heating back to above  $T_C$ . The temperature-dependent remnant strain appearing in the ferroelectric phase increases nonlinearly with applied force, and the difference between the temperature-dependent bending deformations for two similar forces shows a gradual decrease with increasing force, which suggests that the strain approaches saturation. Figure 4 shows the remnant strain at room temperature versus each given applied force and the corresponding stress. The values of remnant strain in figure 4 were obtained from figure 3 by calculating with the bending deformation for each given applied force at room temperature after deduction of elastic component. It is observed that the remnant strain increases nonlinearly with applied stress and inclines to saturation when the stress is larger than 4.5 MPa. According to the stress-strain curve measured directly at room temperature on a rhombohedral PZT ceramics [19], the value of stress to get saturation is about 100 MPa and the remnant strain is about 0.55% for 500 MPa applied stress, but, in our case, the strain is getting to saturation at 4.5 MPa and remnant strain is 0.16% obtained under 9 MPa applied stress. This indicates that macroscopic remnant strain can be induced easily by cooling through  $T_C$  under a small applied force, which is discussed later.

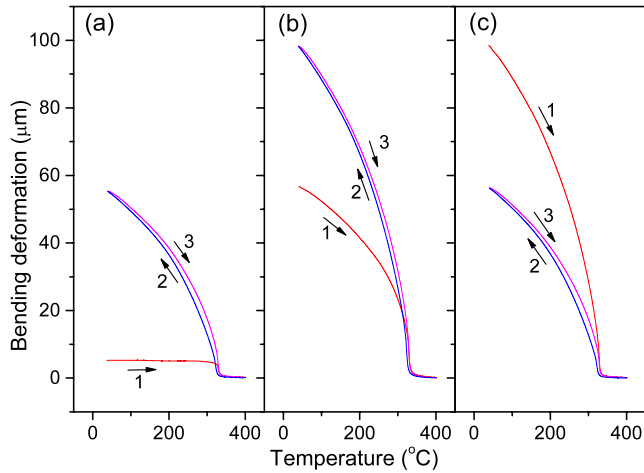


**Figure 5.** The bending deformation as function of temperature for the sample PLZT01 under various history states. (a) Measured at 200 mN after zero force cooling, (b) measured at 600 mN after force cooling with 200 mN, (c) measured at 200 mN after force cooling with 600 mN. The numbers are to mark the sequence of thermal run.

Moreover, a history effect of the remnant strain for a mechanically poled sample is observed, as shown in figure 5, where all the measurements are started on heating from room temperature and go through a subsequent thermal cycle. In each measurement, the applied force is constant, and it is seen that the value of bending deformation during the initial heating run is independent of the current applied force but equal to that generated from the historical value applied during the previous cooling process. At first, the initial annealed sample was loaded with 200 mN applied dynamic force and the temperature-dependent bending deformation is shown in figure 5(a); during the initial heating run, the bending deformation is very small and it is mainly attributed to the elastic strain, so the ferroelastic domain switching is almost non-existent, whereas, on the subsequent cooling, a large bending deformation occurs below  $T_C$  and it is repeatable in the following thermal runs. Thereon, the 200 mN poled sample was poled with 600 mN force (result is shown in figure 5(b)); on the first heating run, the bending deformation is equal to the value generated for 200 mN rather than that expected for 600 mN, and then, during cooling, the bending deformation goes to the amplitude expected for 600 mN. Finally, the 600 mN poled sample was poled with 200 mN force again; as shown in figure 5(c). On the initial heating run, the bending deformation is same as that seen for 600 mN, and during cooling it reverts to the value for 200 mN.

During cooling the sample from the paraelastic into the ferroelastic phase, a large remnant strain can be easily induced by applying a force, and the value of remnant strain depends on the force and temperature. But, during heating back to paraelastic phase, the remnant strain is unchanged by applying a force, even when it is much larger than the force used during previous cooling, and it just depends on temperature disappearing completely at above  $T_C$ . This indicates that the remnant strain is almost independent of the force applied during heating but it does depend on its mechanical history.

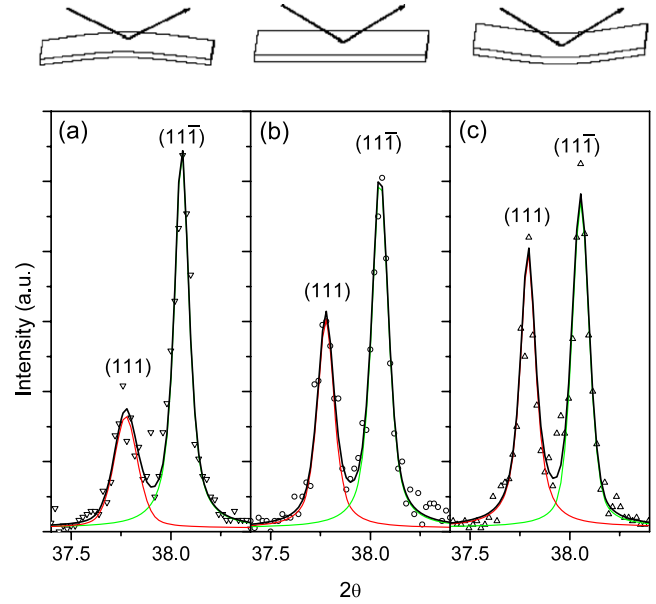


**Figure 6.** Comparison of the x-ray diffraction intensities of the pseudocubic (111) and  $(11\bar{1})$  reflections measured on the bottom of a 600 mN poled sample (a), an initial sample (b), and the top of the 600 mN poled sample (c). The results were fitted with the software of Fullprof. The corresponding set-up for x-ray measurements are schematically shown above the graph.

Therefore, at low mechanical stress (such as the force used in this study which could be lower than the coercive field of ferroelastic switching), ferroelastic domain switching is not easily activated in the ferroelectric sample unless it is cooled from above  $T_C$  under an applied force. The history effect is further explained in terms of the formation of specific state of non-180° domain walls below.

#### 4.3. Non-180° domain switching

Figure 6 shows a comparison of the intensities of the pseudocubic (111) and  $(11\bar{1})$  reflections measured on the bottom of a 600 mN poled sample, an initial sample, and the top surface of the 600 mN poled sample, respectively. The result for the bottom surface of the poled sample shows that the intensity of (111) reflection is decreased and the intensity of  $(11\bar{1})$  reflection is increased; however, the intensities measured from the top surface are biased in the opposite sense. The intensity ratio  $I_{(11\bar{1})}/I_{(111)}$  for the initial sample is 1.68, and after mechanical poling the intensity ratios for the bottom and top surfaces are modified to 2.56 and 1.20, respectively. Here, it should be mentioned that the hot-pressed sintered ceramic sample has a preferred orientation because the intensity ratio for the initial sample is different from the value of 2.94 measured from a randomly-oriented powder sample. The observed variation of the intensity ratios for the mechanically poled sample indicates that non-180° domain switching has occurred during mechanical poling. In the three-point bending mode, as a bending force is applied on the sample, internal stresses acting in the sample lie parallel to the length of the sample; the top region of the sample is put into compression and the bottom region of the sample is put

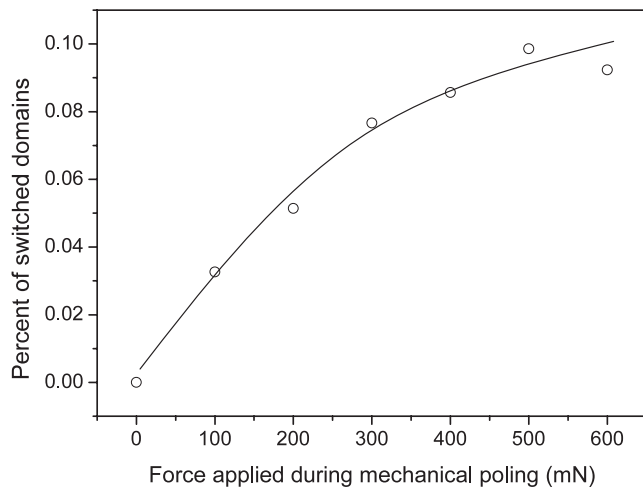


**Figure 7.** Fraction of non-180° switched domains calculated from x-ray diffraction results measured on the bottom surface of the PLZT01 sample after mechanical poling with various applied forces. The line is a guide to the eye.

into tension. Therefore, the non-180° domain switching in the top and bottom surfaces of the poled sample occur in two different ways. According to the equation (2), the calculated fractions of non-180° switched domains in the bottom and top surfaces of the mechanical poled sample are 9.2% and -8.1%, respectively. The positive percentage means that a fraction of the domains in the bottom of the sample align their polar axis away from perpendicular to the sample surface under tensile stress and the negative one corresponds to a fraction of domains in the top of the sample that switch their polar axis to be perpendicular to the sample surface under compressive stress.

Furthermore, x-ray diffraction patterns have been measured from the bottom of the sample after each mechanical poling measurement under various applied forces, and the effect of the applied force on the non-180° domain switching is obtained by analyzing the variation of the intensities of (111) and (11 $\bar{1}$ ) diffraction peaks. The fraction of non-180° domain switching has been calculated from the intensity ratio of the (111) and (11 $\bar{1}$ ) reflections, and is plotted as a function of applied force in figure 7. It can be seen that the fraction of non-180° switched domains increases nonlinearly with the applied forces. As the force increases to larger than 300 mN, the fraction of switched domains begins to show a smaller increase with force and tends to saturate, which is very consistent with the saturation behavior of remnant strain shown in figure 4.

As a PZT sample is cooled through the paraelectric-ferroelectric phase transition, 180° and non-180° domain walls are formed to minimize the electrostatic energy of depolarizing fields and the elastic energy associated with mechanical constraints. If an external mechanical stress is applied on the sample during cooling, more unit cells will align their long dipole axis perpendicular to the compression stress and parallel to the tensile stress by non-180° domain switching. This means that the population of domains with a polar axis parallel to the stress is increased under tensile stress and decreased under compression stress. Analogous behaviors of the non-180° domain switching have been reported by *in situ*

x-ray diffraction measurements at room temperature during applied tensile or compressive stress on PZT ceramics [9, 12]. However, when we keep the PZT sample at a temperature below  $T_C$ , no obvious remnant strain can be observed under an applied force limited in our range of studies, but significant remnant strain can be obtained by the mechanical poling during cooling. Therefore, it is expected that, when cooling a sample under external mechanical stress, to minimize the elastic energy, more non-180° domain walls are formed during the ferroic phase transition, compared with that on zero force cooling. The formation of larger number of non-180° domain walls will give rise to a remnant strain and facilitate the ferroelastic domain switching (i.e. the movement of non-180° domain walls), so larger macroscopic remnant strain can be induced more easily when cooling under an applied force. The specific state of non-180° domain walls formed upon para-ferroelastic phase transition at each applied forces would be different and it can be memorized until it is reset by heating over  $T_C$ , which results in the history effect described above. Binder *et al* [37] has indicated that domain states reached by force cooling from the paraelastic phase into the ferroelastic phase are more close to thermal equilibrium than that by applied field within the ferroelastic phase. Harrison *et al* [38] also found that the repeated heating and cooling through the transition yielded a domain configuration most favorable for super elasticity in LaAlO<sub>3</sub>.

## 5. Conclusions

Temperature-dependent remnant strain has been measured on La-modified PZT ceramics including normal and relaxor ferroelectrics. The ferroelastic phase transition and shape memory effect are demonstrated directly by the evolutions of the remnant strain. X-ray diffraction measurements have demonstrated that non-180° domain switching gives rise to the macroscopic strain and an expression to calculate the percentage of non-180° switched domains for rhombohedral ferroelectrics has been derived. Moreover, the observed history effect is ascribed to a specific domain state formed during the para-ferroelastic phase transition under applied force.

## Acknowledgments

This work was supported by NERC in the form of grant, number NER/A/S/2003/00537. One of the authors (FA) is indebted to the Spanish Ministerio de Educación y Ciencia (MEC) for a postdoctoral research grant.

## References

- [1] Liu J Y, Rogan R C, Ustundag E and Bhattacharya K 2005 *Nat. Mater.* **4** 776
- [2] Menou N, Muller C, Baturin I S, Shur V Y and Hodeau J L 2005 *J. Appl. Phys.* **97** 064108
- [3] Liu M and Hsia K J 2003 *Appl. Phys. Lett.* **83** 3978
- [4] Ma W H and Cross L E 2005 *Appl. Phys. Lett.* **86** 072905
- [5] Cho Y C, Park S E, Cho C R and Jeong S Y 2005 *Appl. Phys. Lett.* **87** 161914

- [6] Catalan G, Janssens A, Rispens G, Csiszar S, Seeck O, Rijnders G, Blank D H A and Noheda I B 2006 *Phys. Rev. Lett.* **96** 127602
- [7] Wang J, Neaton J B, Zheng H, Nagarajan V, Ogale S B, Liu B, Viehland D, Vaithyanathan V, Schlom D G, Waghmare U V, Spaldin N A, Rabe K M, Wuttig M and Ramesh R 2003 *Science* **299** 1729
- [8] Eerensteini W, Wiora M, Prieto J L, Scott J F and Mathur N D 2007 *Nat. Mater.* **6** 348
- [9] Rogan R C, Ustundag E, Clausen B and Daymond M R 2003 *J. Appl. Phys.* **93** 4104
- [10] Hall D A, Steuwer A, Cherdhirunkorn B, Mori T and Withers P J 2004 *J. Appl. Phys.* **96** 4245
- [11] Menou N, Muller C, Baturin I S, Shur V Y and Hodeau J L 2005 *J. Appl. Phys.* **97** 064108
- [12] Glazounov A E, Kungl H, Reszat J T, Hoffmann M J, Kolleck A, Schneider G A and Wroblewski T 2001 *J. Am. Ceram. Soc.* **84** 2921
- [13] Jones J L, Slamovich E B, Bowman K J and Lupascu D C 2005 *J. Appl. Phys.* **98** 104102
- [14] Jones J L, Slamovich E B and Bowman K J 2005 *J. Appl. Phys.* **97** 034113
- [15] Zhang X, Li C and Chen K 2005 *J. Am. Ceram. Soc.* **88** 335
- [16] Pruvost S, Lebrun L, Sebald G, Seveyrat L, Guyomar D, Zhang S and Shrout T R 2006 *J. Appl. Phys.* **100** 074104
- [17] Bedoya C, Muller C, Baudour J L, Madigou V, Anne M and Roubin M 2000 *Mater. Sci. Eng. B* **75** 43
- [18] Guo R, Cross L E, Park S E, Noheda B, Cox D E and Shirane G 2000 *Phys. Rev. Lett.* **84** 5423
- [19] Schaufele A B and Hardtl K H 1996 *J. Am. Ceram. Soc.* **79** 2637
- [20] Vielend D, Jang S J, Cross L E and Wutting M 1991 *J. Appl. Phys.* **69** 6595
- [21] Wang C, Redfern S A T, Daraktchiev M and Harrison R J 2006 *Appl. Phys. Lett.* **89** 152906
- [22] Wang C, Aguado F and Redfern S A T 2007 *Appl. Phys. Lett.* **91** 192908
- [23] Als-Nielsen J and McMorrow D 2001 *Elements of Modern X-Ray Physics* (New York: Wiley) p 246
- [24] Do D, Evans P G, Isaacs E D, Kim D M, Eom C B and Dufresne E M 2004 *Nat. Mater.* **3** 365
- [25] Subbarao E C, Mcquarrie M C and Buessem W R 1957 *J. Appl. Phys.* **28** 1194
- [26] Bokov A A and Ye Z G 2006 *J. Mater. Sci.* **41** 31
- [27] Dai X, Xu Z, Li J F and Viehland D 1996 *J. Mater. Res.* **11** 618
- [28] Cordero F, Corti M, Cracium F, Galassi C, Piazza D and Tabak F 2005 *Phys. Rev. B* **71** 094112
- [29] Jimenez B and Vicente J M 1998 *J. Phys. D: Appl. Phys.* **31** 130
- [30] Bourim E M, Tanaka H, Gabbay M, Fantozzi G and Cheng B L 2002 *J. Appl. Phys.* **91** 6662
- [31] Wang C, Fang Q F, Shi Y and Zhu Z G 2001 *Mater. Res. Bull.* **36** 2657
- [32] Wang C, Fang Q F and Zhu Z G 2002 *J. Phys. D: Appl. Phys.* **35** 1545
- [33] Jimenez B and Jimenez R 2002 *Phys. Rev. B* **66** 014104
- [34] Pandit P, Gupta S M and Wadhawan V K 2004 *Solid State Commun.* **131** 665
- [35] Pandit P, Gupta S M and Wadhawan V K 2006 *Smart Mater. Struct.* **15** 653
- [36] Jimenez B and Vicente J M 2000 *J. Phys. D: Appl. Phys.* **33** 1525
- [37] Binder A and Knorr K 2000 *Phys. Rev. B* **61** 190
- [38] Harrison R J, Redfern S A T and Salje E K H 2004 *Phys. Rev. B* **69** 144101